Preparation of Nanometer-Sized Manganese Oxides by Intercalation of Organic Ammonium Ions in Synthetic Birnessite OL-1

Qiuming Gao, Oscar Giraldo, Wei Tong, and Steven L. Suib*

Department of Chemistry, Box U-60, Department of Chemical Engineering and Institute of Materials Science, University of Connecticut, Storrs, Connecticut 06269-4060

Received May 25, 2000. Revised Manuscript Received November 21, 2000

Potassium manganese oxide materials having the synthetic birnessite structure K-OL-1 were synthesized by reduction methods. K-OL-1 has been ion-exchanged with H^+ to produce H-OL-1, which was utilized in further intercalating reactions. The tetraalkylammonium hydroxides including tetramethylammonium hydroxide, tetraethylammonium hydroxide, tetrapropylammonium hydroxide, and tetrabutylammonium hydroxide and diamines such as ethylenediamine, 1,6-diaminohexane, and 1,10-diaminooctane were used to intercalate H-OL-1. Elemental analyses, X-ray diffraction, FT-IR spectroscopy, scanning electron microscopy and energy-dispersive X-ray analysis, UV−vis spectroscopy, and transmission electron microscopy have been used to characterize the samples. Structural models of both wet and dry samples are given. The intercalation and deaquation processes of TAA and DA-OL-1 were studied. Their particle sizes were determined and nanometer-sized TAA-OL-1 samples were prepared in TAA systems.

Introduction

Considerable research has recently focused on manganese oxides, due to their ion-exchange, molecular adsorption, catalytic, electrochemical, and magnetic properties.[1−8] Birnessite is a two-dimensional layered structure, comprised of edge shared MnO_6 octahedra, with water molecules and/or metal cations occupying the interlayer region.[9−15] Natural birnessite exists widely in deep-sea nodules and in soils in some areas.[9,16−18] The syntheses of birnessite have usually been carried out by three methods: oxidation of Mn^{2+},[19−21] reduction of permanganate MnO_4^-,[1,22−24] and redox reactions between Mn^{2+} and MnO_4^-.[25−28] Other methods have also been reported.[13,29−31]

The development of nanomaterials and preparation of films are general areas of concern to researchers.[32−43]

(1) Shen, Y. F.; Zerger, R. P.; DeGuzman, R. N.; Suib, S. L.; McCurdy, L.; Potter, D. I.; O'Young, C. L. *Science* **1993**, *260*, 511.
(2) (a) Feng, Q.; Karoh, H.; Miyai, Y.; Ooi, K. *Chem. Mater.* **1995**, *7*, 148. (b) Feng, Q.; Kanoh, H.; Miyai, Y.; Ooi, K. *Chem. Mater.* **1995**, *7*, 1226. (c) Feng, Q.; Kanoh, H.; Miyai, Y.; Ooi, K. *Chem. Mater.* **1995**, *7*, 1722.
(3) Tsuji, M.; Abe, M. *Solvent Extr. Ion Exch.* **1984**, *2*, 253.
(4) Yin, Y. G.; Xu, W. Q.; Shen, Y. F.; Suib, S. L. *Chem. Mater.* **1994**, *6*, 1808.
(5) Koksbang, R.; Barker, J.; Shi, H.; Saidi, M. Y. *Solid State Ionics* **1996**, *84*, 1.
(6) Feng, Q.; Kanoh, H.; Ooi, K.; Tani, M.; Nakacho, Y. *J. Electrochem. Soc.* **1994**, *141*, L135.
(7) Armstrong, A. R.; Bruce, P. G. *Nature* **1996**, *381*, 499.
(8) Rao, C. N. R.; Cheetham, A. K.; Mahesh, R. *Chem. Mater.* **1997**, *8*, 22421.
(9) Bricker, O. *Am. Mineral.* **1965**, *50*, 1296.
(10) Pereira-Ramos, J. P.; Badour, R.; Bach, S.; Bafier, N. *Solid State Inoics* **1992**, *701*, 3.
(11) Bach, S.; Pereira-Ramos, J. P.; Baffier, N. *Electrochim. Acta* **1993,** *38*, 1995.
(12) Bach, S.; Pereira-Ramos, J. P.; Baffier, N. *J. Solid State Chem.* **1995**, *120*, 70.
(13) Bach, S.; Henry, M.; Baffier, N.; Livage, J. *J. Solid State Chem.* **1990**, *88*, 325.
(14) Parent, J.; Olazcuaga, R.; Devalette, M.; Fouassier, C.; Hagenmuller, P. *J. Solid State Chem.* **1971**, *3*, 1.
(15) Baser, W.; Graf, P.; Feitknecht, W. *Helv. Chim. Acta* **1954**, *37*, 2322.
(16) (a) Turner, S.; Buseck, P. R. *Science* **1979**, *203*, 456. (b) Turner, S.; Buseck, P. R. *Science* **1981**, *212*, 1024. (c) Siegel, M. D.; Turner, S. *Science* **1983**, *219*, 172.
(17) Taylor, R. M.; Mckenzie, R. M.; Norrish, K. *Aust. J. Soil Res.* **1964**, *2*, 235.
(18) Chukhiov, F. V.; Gorshkov, A. I. *Trans. R. Soc. Edinburgh* **1981**, *72*, 195.
(19) Golden, D. C.; Chen, C. C.; Dixon, J. B. *Clays Clay Miner.* **1987**, *35*, 271.
(20) Giovanoli, R.; Stahli, E.; Feitknecht, W. *Helv. Chim. Acta* **1970**, *53*, 209.
(21) Feitknecht, W.; Marti, W. *Helv. Chim. Acta* **1945**, *28*, 129.
(22) Ching, S.; Landrigan, J. A.; Jorgensen, M. L.; Duan, N.; Suib, S. L. *Inorg. Chem.* **1997**, *36*, 883.
(23) Ching, S.; Landrigan, J. A.; Jorgensen, M. L.; Duan, N., Suib, S. L. *Chem. Mater.* **1995**, *7*, 1604.
(24) McMurdie, H. F. *Trans. Electrochem. Soc.* **1944**, *86*, 313.
(25) Shen, Y. F.; Suib, S. L.; O'Young, C. L. *J. Am. Chem. Soc.* **1994**, *116*, 11020.
(26) Luo, J.; Suib, S. L. *J. Phys. Chem. B* **1997**, *101*, 10403.
(27) Luo, J.; Huang, A.; Park, S.; Suib, S. L. *Chem. Mater.* **1998**, *10*, 1561.
(28) Shen, Y. F.; Zerger, R. P.; DeGuzman, R. N.; Suib, S. L.; McCurdy, L.; Potter, D. I.; O'Young, C. L. *J. Chem. Soc., Chem. Commun.* **1992**, 1213.
(29) Le Goff, P.; Baffier, N.; Bach, S.; Pereira-Ramos, J. P.; Messina, R. *Solid State Ionics* **1993**, *61*, 309.
(30) Kanoh, H.; Tang, W.; Makita, Y.; Ooi, K. *Langmuir* **1997**, *13*, 6845.
(31) Perei-Ramos, J. P.; Badour, R.; Bach, S.; Baffier, N. *Solid State Ionics* **1992**, *701*, 3.
(32) Kaschak, D. M.; Johnson, S. A.; Hoks, D. E.; Kim, H. N.; Ward, M. D.; Mallouk, T. E. *J. Am. Chem. Soc.* **1998**, *120*, 10887.
(33) Krishnamoorti, R.; Vaia, R. A.; Giannelis, E. *Chem. Mater.* **1996**, *8*, 1728.
(34) Lemmon, J. P.; Lerner, M. M. *Chem. Mater.* **1994**, *6*, 207.
(35) (a) Tsai, H. L.; Heising, J.; Schindler, J. L.; Kannewurf, C. R.; Kanatzidis, M. G. *Chem. Mater.* **1997**, *9*, 879. (b) Tsai, H. L.; Schindler, J. L.; Kannewurf, C. R.; Kanatzidis, M. G. *Chem. Mater.* **1997**, *9*, 875.
(36) Brousseau, L. C.; Aurentz, D. J.; Benesi, A. J.; Mallouk, T. E. *Anal. Chem.* **1997**, *69*, 688.

10.1021/cm000426c CCC: $20.00
Published on Web 02/14/2001

The preparation of nanometer-sized manganese oxide colloids with mean particle sizes of 5.6 nm has been carried out by using a two-step method.[44] Tetraalkylammonium ions were chosen to react with potassium permanganate to form tetraalkylammonium permanganates, which were reduced by 2-propanol water mixtures. Structural model studies showed the presence of birnessite inorganic layers with the tetraalkylammonium ions intercalated into the layers. The very recent work of Ooi et al.[45] showed that tetraalkylammonium ions were able to intercalate directly into the layers of birnessite by ion-exchange methods, similar to other layered structures, such as zirconium phosphates[32] and montmorillonite clays.[43] The distribution of water molecules and ammonium ions between the layers was different from our results,[44] showing the complexity of these systems. The research reported here involves structural models, intercalation, deaquation processes, and particle size control of birnessite directly intercalated by tetraalkylammonium ions and diammonium ions.

Experimental Section

Chemicals. Potassium permanganate (99.0%) was purchased from Alfa. Amines are commercially available from Aldrich and Alfa and were used as received. The amines include tetramethylammonium hydroxide (25 wt % solution, Aldrich), tetraethylammonium hydroxide (35 wt % solution, Aldrich), tetrapropylammonium hydroxide (1.0 M solution, Alfa), tetrabutylammonium hydroxide (40 wt % solution, Aldrich), ethylenediamine (98%, Aldrich), 1,6-diaminohexane (99%, Aldrich), and 1,10-diaminooctane (98%, Aldrich).

Preparation of K-OL-1 and H-OL-1. Potassium type manganese oxide birnessite K-OL-1 was synthesized by reduction methods.[46] The 200 mL solution of the mixture of 92.0 mL of ethanol and 33.6 g of potassium hydroxide was added slowly to a beaker containing a 150 mL solution of 9.48 g of potassium permanganate with vigorous stirring for 1 h. The resultant gel was aged at 80 °C in an oven for 48 h. The product was washed with distilled deionized water (DDW) to a pH lower than 9. Still wet, this sample was transferred into a beaker which contained 200 mL of 1.0 M HNO_3 and stirred at ambient temperature for 24 h. In a similar way, K-OL-1 was ion-exchanged with H^+ three times to make sure the ion-exchange reaction was complete. The product was washed with DDW to a pH higher than 6. Kept wet, the H-OL-1 sample was used for further intercalation reactions.

Organic Amines or Ammoniums Intercalation Reaction. The tetraalkylammonium hydroxides (TAA) including tetramethylammonium hydroxide (TMA), tetraethylammonium hydroxide (TEA), tetrapropylammonium hydroxide (TPA), and tetrabutylammonium hydroxide (TBA) and diamines (DA) like ethylenediamine (en), 1,6-diaminohexane (1,6-DHA), and 1,10-diaminooctane (1,10-DOA) were used to intercalate into the layers of H-OL-1. The 0.015 mol of TAA or DA was added to the gel (50 mL including 0.015 mol of Mn) of H-OL-1. The whole mixture was stirred for certain times and the resultant colloids or gels were characterized.

Elemental Analysis. The manganese and potassium amounts were determined with a Perkin-Elmer model 2380 flame absorption spectrometer and model P 40 inductively coupled plasma with an atomic emission spectrometer (ICP-AES).

X-ray Diffraction. A Scintag XDS-2000 diffractometer utilizing Cu Kα radiation with a voltage of 45 kV and current of 40 mA was used to obtain diffraction patterns. Samples were prepared by pipetting small amounts of the sols/colloids onto glass slides and allowing the solvent to evaporate for a certain time at ambient temperature.

FT-IR Spectroscopy. The FT-IR spectra were taken on a Nicolet Magna-IR System 750 FT-IR spectrometer, using standard KBr pellet methods.

Scanning Electron Microscopy and Energy-Dispersive X-ray Analysis (SEM-EDX). SEM photographs were taken on an Amray 1810 scanning electron microscope. An Amray model PV 9800 EDX system was used to obtain energy-dispersive X-ray analyses.

UV−Vis Spectroscopy. A HP 8452A spectrophotometer was used to obtain the UV−vis spectra, using 1.0 cm quartz cells. The sols/colloids were diluted to concentrations of 10^{-3}−10^{-4} mol L^{-1} Mn for the measurements.

Transmission Electron Microscopy (TEM). Samples were prepared by placing a drop of 10^{-2}−10^{-3} mol L^{-1} Mn sols/colloids on carbon coated copper grids and allowing the water to evaporate at ambient temperature. TEM images were obtained at 100 kV with a Philips EM 420 electron microscope.

Results and Discussion

1. Characterization of K-OL-1 and H-OL-1. Potassium type OL-1 (K-OL-1) was not active for ion-exchange reactions of organic ammonium ions, similar to sodium type OL-1 (Na-OL-1). Ion-exchange methods were chosen to prepare proton type birnessite (H-OL-1). XRD analyses of K-OL-1 prepared by reduction methods and proton ion-exchanged H-OL-1 showed that the layered structures had a basal spacing of 0.72 nm. The radii of H_3O^+ and K^+ are similar, H_3O^+ ions occupy the K^+ ion positions of K-OL-1, so the interlayer distances of K-OL-1 and H-OL-1 are very similar. SEM images of them were given in Figure 1. Both samples were platelike forms without any amorphous or other kinds of crystallized phases, showing that they were pure birnessite. ICP and EDX analyses showed that H-OL-1 included trace K with a K/Mn ratio of 0.02, much lower than that of K-OL-1, whose K/Mn ratio was 0.31. These data showed that most potassium cations K^+ of K-OL-1 were ion-exchanged by protons to form H-OL-1. Potassium ions intercalated between the layers of birnessite were not able to be totally ion-exchanged by protons, based on thermodynamic calculations.[45] More than 93% potassium of the original potassium type K-OL-1 samples was ion-exchanged by protons. These results are similar to results of proton ion-exchanged Na-OL-1 birnessite.[45]

2. Ion-Exchange Reactions and X-ray Diffraction Analyses for TAA- and DA-OL-1. Proton type H-OL-1 was used as a source of birnessite for the ion-exchange reaction between organic ammonium ions and protons in the layers of birnessite. DA first reacted with protons of H-OL-1 forming diammonium cations, as observed

(37) Mallouk, T. E.; Gavin, J. A. *Acc. Chem. Res.* **1998**, *31*, 209.
(38) Kleinfeld, E. R.; Ferguson, G. S. *Chem. Mater.* **1995**, *7*, 2329.
(39) (a) Colon, J. L.; Yang, C. Y.; Clearfield, A.; Martin, C. R. *J. Phys. Chem.* **1988**, *92*, 5777. (b) Colon, J. L.; Yang, C. Y.; Clearfield, A.; Martin, C. R. *J. Phys. Chem.* **1990**, *94*, 874.
(40) Kijima, T.; Matsui, Y. *Nature* **1986**, *322*, 533.
(41) Ding, Y.; Jones, D. J.; Maireles-Torres, P.; Roziere, *J. Chem. Mater.* **1995**, *7*, 562.
(42) Kumar, C. V.; McLendon, G. L. *Chem. Mater.* **1997**, *9*, 863.
(43) Pinnavaia, T. J.; Lan, T.; Wang, Z.; Shi, H. Z.; Kaviratna, P. D. *Nanotechnology*; Crandall, B. C., Ed.; MIT Press: Cambridge, MA, 1996; Chapter 17, p 251.
(44) Brock, S. L.; Sanabria, M.; Suib, S. L.; Urban, V.; Thiyagarajan, P.; Dotter, D. I. *J. Phys. Chem. B* **1999**, *103*, 7416. (Model I assumes the absence of a hydration layer between the TAA cations and manganese oxide layers, although water molecules may be present in the same plane as the TAA cations, model II corresponds to a total of one effective layer of water in addition to the TAA cations, and model III presents an expansion of two layers of water between the TAA cations and the manganese oxide slabs.)
(45) Liu, Z. H.; Ooi, K.; Kanoh, H.; Tang, W. P.; Tomida, T. *Langmuir* **2000**, *16*, 4154.
(46) Ma, Y.; Luo, J.; Suib, S. L. *Chem. Mater.* **1999**, *11*, 1972.

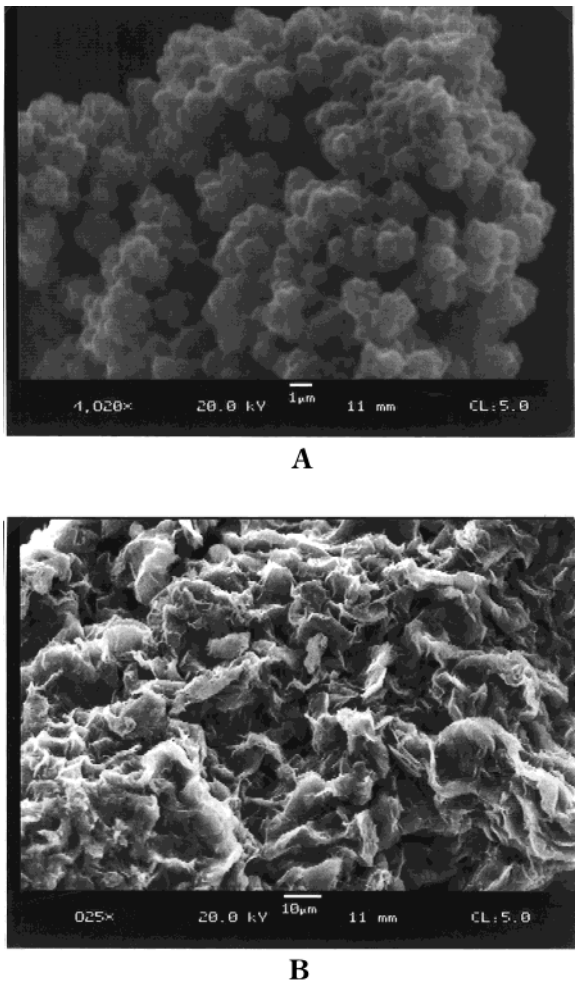

Figure 1. Scanning electron microscopy images of potassium type birnessite K-OL-1 (A) and proton ion-exchanged birnessite H-OL-1 (B).

with other TAA cations. These processes were followed by FT-IR spectroscopy. Absorption bands characteristic of NH_3^+ were clearly observed, instead of NH_2, for all of the dried TAA-OL-1 and DA-OL-1 samples.

All of the ion-exchange reactions have been carried out for 3 days at ambient temperature to make sure the intercalation was complete. The XRD patterns of TMA intercalated samples (Figure 2) showed a very complex pattern compared with other members of the TAA-OL-1 system. These peaks could not be indexed to any known structure. OL-1 inorganic layers kept their original structures under intercalation conditions. The coexistence of two kinds of structures with different layer distances is likely. The peaks at 2.58, 0.86, 0.62, and 0.48 nm were indexed to the (001), (003), (004), and (005) reflections of the structure, respectively, using a trigonal or hexagonal crystal system.[44] The *d*-values of the (001) crystal spacing reflections are related to the interlayer distances, so the interlayer distance of this structure is 2.58 nm. This structure was a little irregular because of the absence of (002) peaks and deviation of others. The others peaks at 1.18, 0.60, 0.40, and 0.30 nm were indexed to the (001), (002), (003), and (004) reflections of the structure, respectively, with interlayer distances of 1.18 nm.

The indexing of the peaks for other TAA intercalated OL-1 materials was described as follows. The peaks at

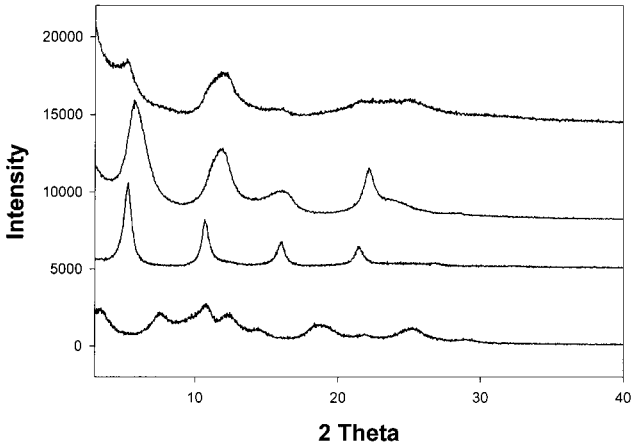

Figure 2. X-ray diffraction patterns of wet tetraalkylammonium ions intercalated into birnessite TAA-OL-1, collected immediately after pipetting small amounts of colloids onto glass slides. XRD patterns for TMA-OL-1 (bottom), TEA-OL-1, TPA-OL-1, and TBA-OL-1 (top).

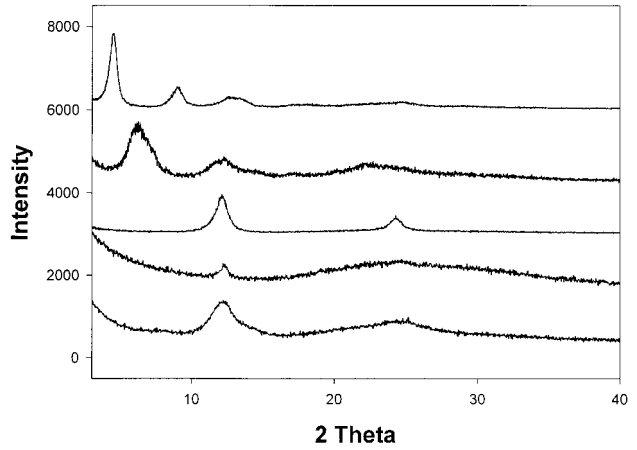

Figure 3. X-ray diffraction patterns of wet diammonium ion intercalated birnessite DA-OL-1, collected immediately after pipetting small amounts of colloids onto glass slides. XRD patterns of K-OL-1 (bottom), H-OL-1, en-OL-1, 1,6-DHA-OL-1, and 1,10-DOA-OL-1 (top).

1.72, 0.86, 0.57, and 0.43 nm corresponded to the (001), (002), (003), and (004) reflections of TEA intercalated OL-1, respectively, with an interlayer distance of 1.72 nm. The peaks at 1.56, 0.78, 0.52, and 0.39 nm were due to (001), (002), (003), and (004) reflections of TPA-OL-1 samples, respectively, with a distance of 1.56 nm. Those at 1.69, 0.85, 0.56, 0.42, and 0.34 nm are related to the (001), (002), (003), (004), and (005) reflections of TBA samples, respectively, with a distance of 1.69 nm.

Figure 3 showed the XRD patterns of DA-OL-1 samples. The X-ray patterns of the K-OL-1 and H-OL-1 phases were also given for comparison with all other X-ray data. The first strong peaks at the lowest two-θ values were shifted to lower two-θ angle positions. The peaks at 0.723 and 0.362 nm correspond to the (001) and (002) reflections of en intercalated OL-1, respectively, with an interlayer distance of 0.723 nm. The peaks at 1.48, 0.74, 0.49, and 0.37 nm were indexed to (001), (002), (003), and (004) reflections, respectively, of 1,6-DHA-OL-1 with an interlayer distance of 1.48 nm. Those peaks at 1.86, 0.93, 0.62, 0.46, and 0.37 were due to (001), (002), (003), (004), and (005) reflections of 1,10-DOA-OL-1, respectively, with an interlayer distance of 1.86 nm.

Table 1. Structural Models of Wet and Dry Samples of Organic Amine or Ammonium Intercalated Manganese Oxides OL-1

cation	cation size, nm	model of wet sample[a]	obsd interlayer spacing of wet sample, nm	model of dry sample[a]	obsd interlayer spacing of dry sample, nm
TBA	0.95−1.05	one layer of TBA and one layer of water (II)	1.69	one layer of water (HOL-1)	0.72
TPA	0.80−0.90	one layer of TPA and one layer of water (II)	1.56	one layer of TPA (I)	1.31
TEA	0.65−0.75	one layer of TEA and two layers of water (III)	1.75	one layer of TEA and two layers of water (III)	1.75
TMA	0.50−0.60	two layers of TMA and three layers of water; one layer of TMA and one layer of water	2.58; 1.18	two layers of TMA and one layer of water	1.79
1,10-DOA	1.65−1.70	60−62°	1.86	60−62°	1.86
1,6-DHA	1.15−.20	64−73°	1.48	64−73°	1.48
en	0.65−0.70	39−41°	0.723	39−41°	0.723

[a] According to sample structural models of TAA-occluded manganese oxide colloids based on zero, one, and two layers of hydration between the cation and manganese oxide layers.[44]

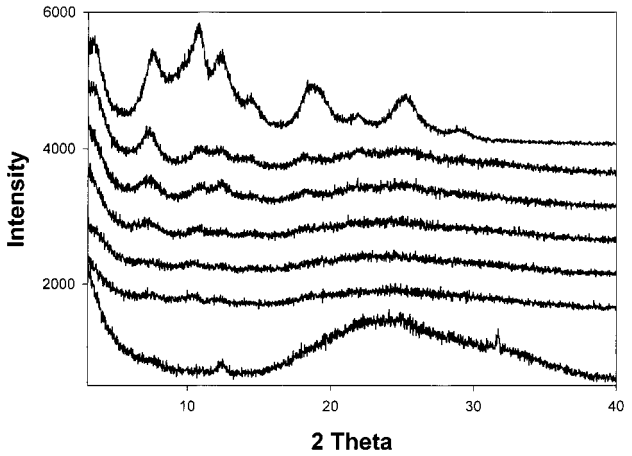

Figure 4. X-ray diffraction patterns of tetramethylammonium ion intercalated OL-1. The gel was stirred for different times at ambient temperature. XRD for samples stirred for 1 (bottom), 2, 3, 4, 5, 6, and 12 h (top).

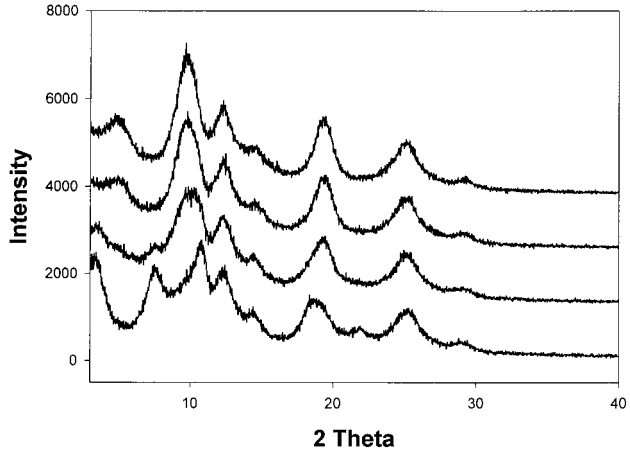

Figure 5. X-ray diffraction patterns of tetramethylammonium ion intercalated OL-1. The gel was stirred for 3 days at ambient temperature. XRD patterns of samples dried for 30 (bottom), 50, 70, and 90 min (top).

Two kinds of organic amines were utilized as intercalating agents, tetraalkylammonium (TAA) hydroxide and diamine (DA), due to their different electronic and steric factors. TMA intercalated H-OL-1 had two kinds of interlayer distances of 2.58 and 1.18 nm. The larger interlayer structure may include two layers of TMA and three layers of water molecules according to diameters of these molecules/ions.[44] The small one included one layer of TMA cations and one layer of water molecules, corresponded to the type II model of TMA manganese oxide prepared by redox methods using tetramethylammonium permanganate.[44] The structures of TEA, TPA, and TBA intercalated H-OL-1 corresponded to those of type III, II, and II models of related structures of redox reactions with TAA permanganates, respectively.[44]

The shorter alkyl chains of TMA lead to more polar and strongly bound TAA cations. The interaction between TMA cations and negatively charged OL-1 inorganic layers was stronger than the others and more and more TMA cations were able to be intercalated into the spaces between the inorganic layers of OL-1. The interaction of TEA was a little weaker than that of TMA, so only one layer of TEA cations and two layers of water molecules were in the layers of OL-1. For TPA and TBA the interactions were much weaker than that of TEA.

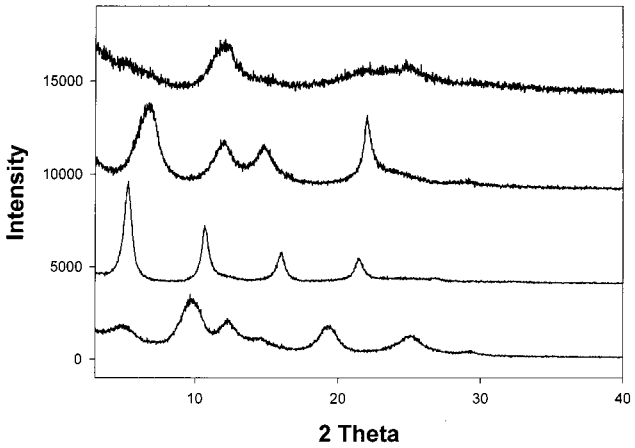

Figure 6. X-ray diffraction patterns of dried tetraalkylammonium ion intercalated OL-1. All TAA-OL-1 samples dried for 1 day. XRD patterns for TMA-OL-1 (bottom), TEA-OL-1, TPA-OL-1, and TBA-OL-1 (top).

Only a structure of one layer of TPA or TBA and one layer of water intercalated into the OL-1 layers was formed (Table 1).

In contrast to the TAA-OL-1 samples, the XRD patterns of diamine intercalated OL-1 had a typical character of intercalated structures with larger interlayer distances that correlate with longer molecular

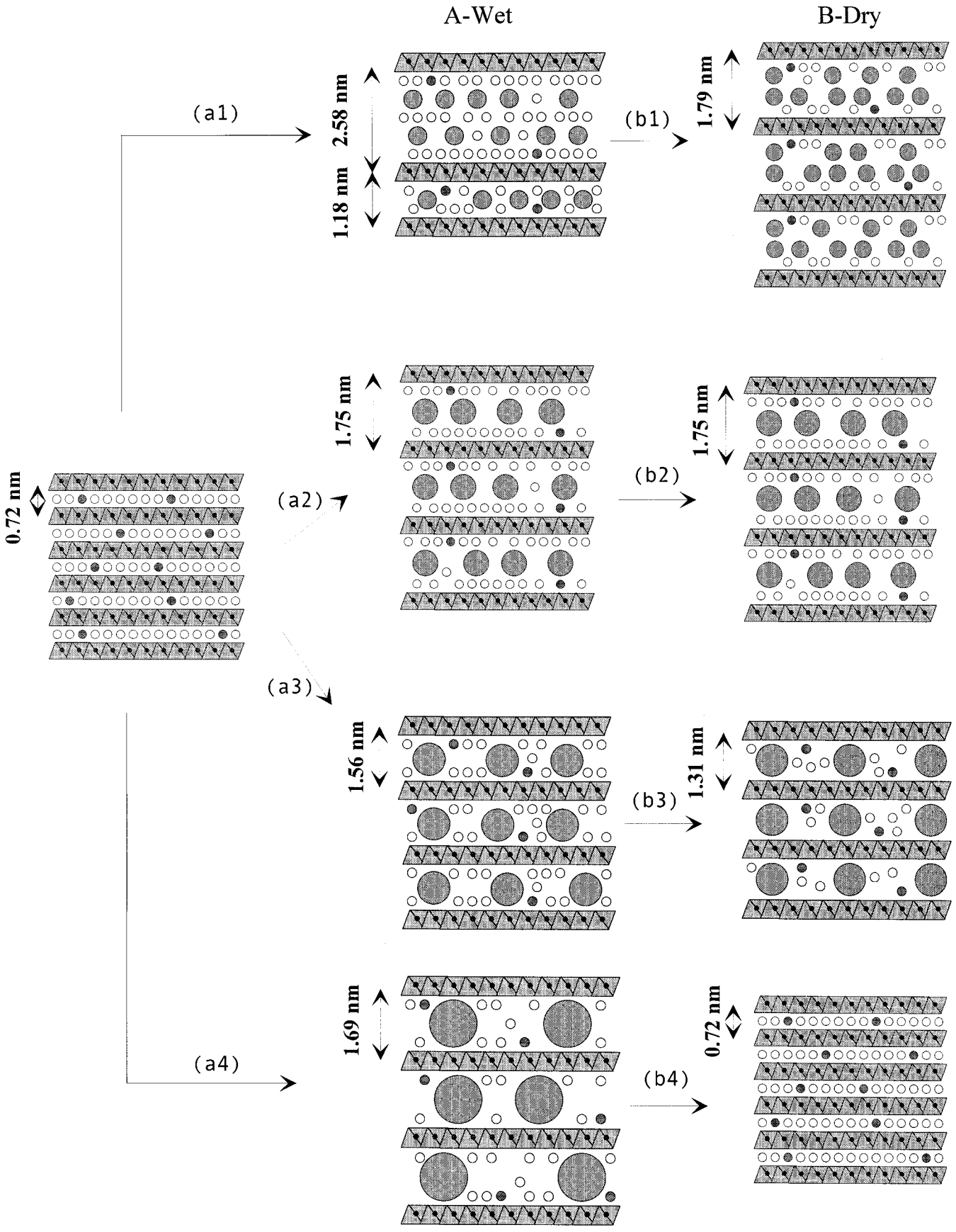

Figure 7. Structural models of tetraakylammonium ions intercalated birnessite TAA-OL-1. (a1) TMA ion intercalated into H-OL-1 and (b1) dried TMA-OL-1; (a2) TEA ion intercalated into H-OL-1 and (b2) dried TEA-OL-1; (a3) TPA ion intercalated into H-OL-1 and (b3) dried TPA-OL-1; (a4) TBA ion intercalated into H-OL-1 and (b4) dried TBA-OL-1. The small white circles represent water molecules, small black circles are potassium ions, and big black circles are TAA cations. The layered black rectangular circles are the manganese oxide layers.

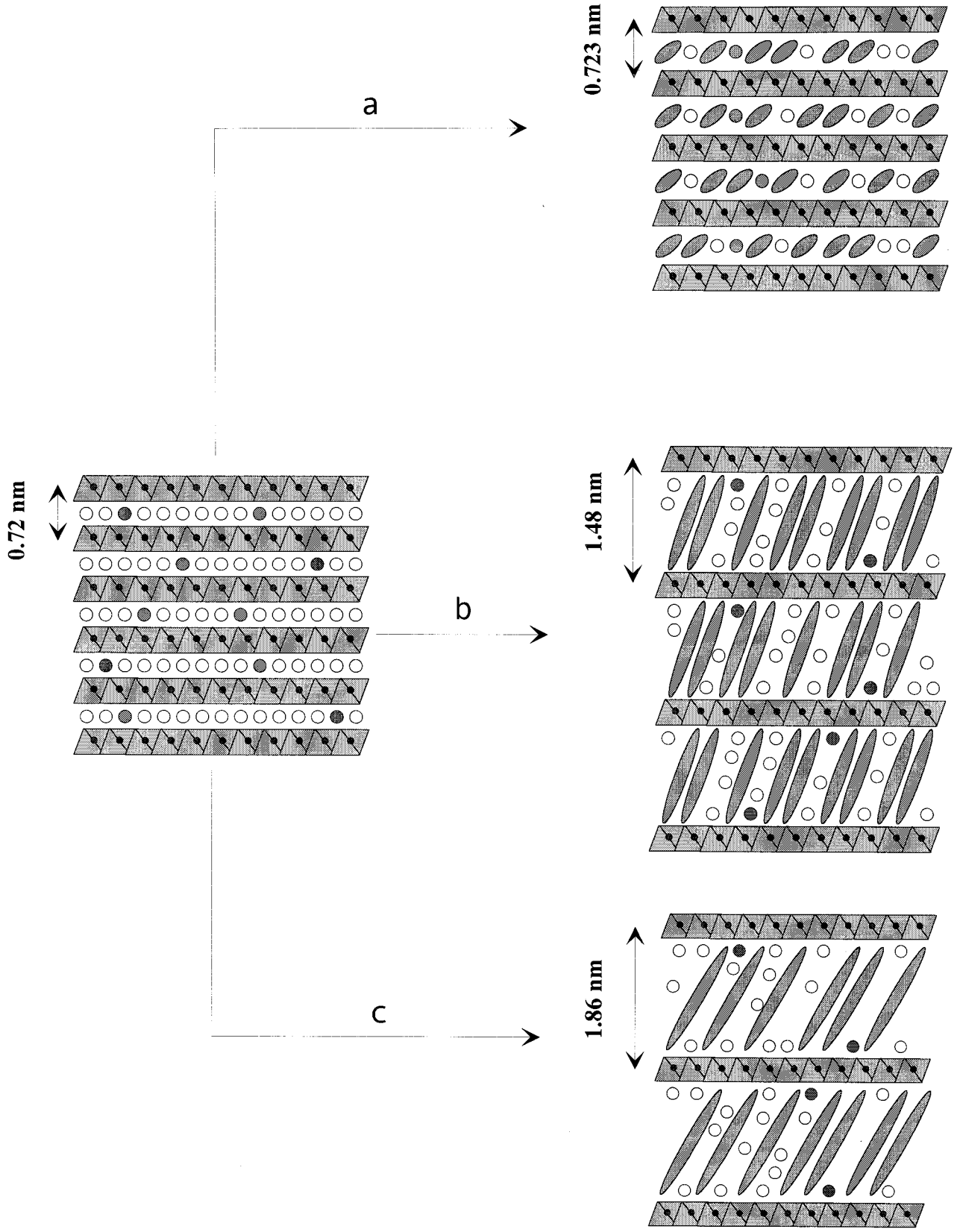

Figure 8. Structural models of diammonium ion intercalated birnessite DA-OL-1. (a) en intercalated into H-OL-1, (b) 1,6-DHA intercalated into H-OL-1, (c) 1,10-DOA-OL-1. XRD patterns of wet and dried states of DA-OL-1 were same. The small white circles represent water molecules, small black circles are potassium ions, and big black circles are TAA cations. The layered black rectangular circles are manganese oxide layers.

distances of different amines. According to C−C, C−N, and N−H bond distances and manganese oxide slab thicknesses, angles of organic ammonium ions between the layers were calculated and these results are also listed in Table 1.

3. Intercalation Processes of TAA- and DA-OL-1. Tetramethylammonium hydroxide was added to the sols of birnessite H-OL-1, with a ratio of ammonium ion/

Table 2. Conditions and Results of UV−Vis Studies of Organic Amine or Ammonium Intercalated Manganese Oxides OL-1

sample	concn of Mn × 10^5, mol L^{-1}	λ_1, nm	ϵ_1 (mol of Mn), $L^{-1}\,cm^{-1} \times 10^4$	λ_2, nm	ϵ_2 (mol of Mn), $L^{-1}\,cm^{-1} \times 10^4$
TMA-OL-1	3.60	216	1.89	368	2.41
TEA-OL-1	4.71	216	1.73	368	2.17
TPA-OL-1	6.20	214	1.50	364	1.98
TBA-OL-1	7.89	216	1.29	370	1.63
en-OL-1	13.66	*a*	*a*	425	0.948
1,6-DHA-OL-1	12.15	*a*	*a*	445	0.884
1,10-DOA-OL-1	15.82	*a*	*a*	445	0.568

[a] UV−vis absorption not observed.

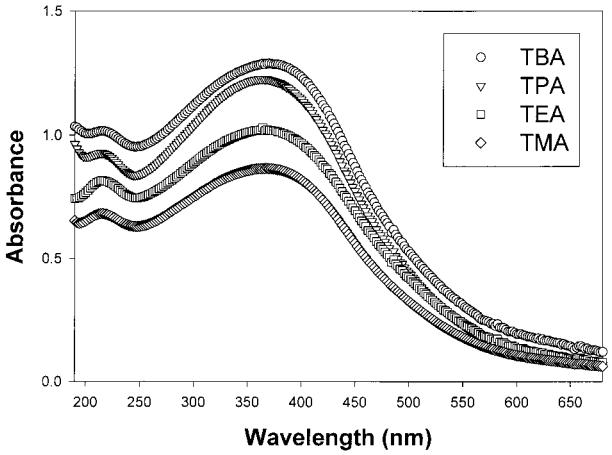

Figure 9. UV−vis spectra of tetraakylammonium ion intercalated OL-1 colloids at room temperature. The samples were diluted to a manganese concentration of 10^{-4}−10^{-3} M.

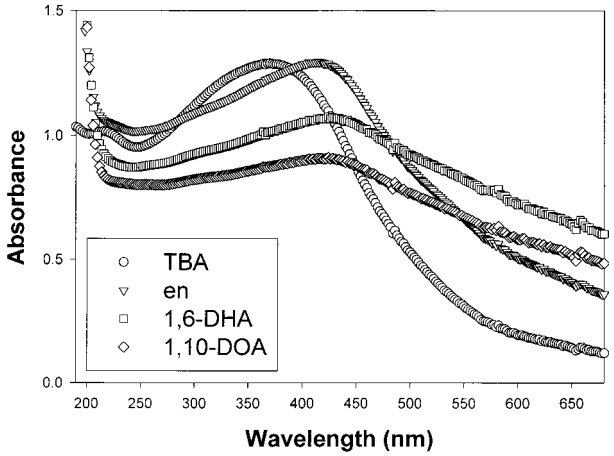

Figure 10. UV−vis spectra of diammonium ion intercalated OL-1 colloids at room temperature. The samples were diluted to a manganese concentration of 10^{-4}−10^{-3} M.

Mn of 1.0. The whole mixture was stirred vigorously for a certain time with the products detected by XRD techniques (Figure 4). One peak at 0.72 nm and a broad peak at about 0.36 nm were found after stirring for 1 h, showing that TMA ions were not intercalated into the layers at this time. After 4 h, a small peak at 1.18 nm was found and became stronger when the mixture was stirred for 5 h. During this period, more TMA entered the layers. Six hours later another peak at 2.58 nm appeared. The intensity of the peak at 1.18 nm increased further at the same time. On further intercalation more and more TMA entered the layers. The intensities and positions of the peaks in the whole XRD pattern were almost stable after 12 h of stirring. Coexistence of structures with an ion-exchange balance of TMA cations was observed at the same time in these colloidal systems.

Intercalation processes for TAA-OL-1 and DA-OL-1 were also carried out. Amines or ammonium ions were intercalated into the layers in about 5 h, similar to that of TMA-OL-1 intercalation. The difference was that there was only one kind of structure formed for other members of this family. The larger sizes of other tetraalkylammonium ions led to only one structure type for other TAA-OL-1 systems. These results further showed that the intercalation was complete after ion-exchange for 3 days at room temperature.

4. Deaquation Processes and Structural Models of Wet and Dried TAA- and DA-OL-1 Samples. The TMA-OL-1 colloids were dropped on a glass fiber, dried for 30 min in air at ambient temperature, and then examined by XRD. Two peaks at 2.58 and 1.18 nm at very low two-θ angles, as well as several other peaks at higher angles, were observed. After 50 min the peak at 2.58 nm shifted to 1.95 nm. Meanwhile, the intensity of the 1.18 nm peak was very weak. The peak at 1.95 nm further shifted to higher angles at 1.79 nm, with the 1.18 nm peak disappearing after drying for 70 min (Figure 5). Then the whole pattern was constant even when the sample was dried for longer time. The XRD patterns of TEA intercalated samples dried for 2 h were the same as those examined immediately after being dropped onto the glass fiber (Figure 6). The TPA-OL-1 and TBA-OL-1 samples dried for 2 h were also examined by XRD.

All of the DA intercalated birnessite OL-1 samples were examined immediately when they were dropped on the glass fibers. After being dried for 2 h, the samples were examined by XRD again and no changes were observed.

When the TMA-OL-1 colloids were dropped on glass fibers, coexisting structures (one including two layers of TMA and three layers of water molecules and one including one layer of TMA cations and one layer of water molecules (type II)) were stable for 50 min, then changed to a new type of layered structure with a spacing of 1.79 nm, which included two layers of TMA and two layers of water analyzed by the same methods (Table 1). Small steric and strong electronic factors of TMA led to a large change in structure of wet and dried materials. The structure type was not changed during the drying processes for TEA intercalated samples, showing a strong interaction between TEA and the OL-1 inorganic layers. TPA-OL-1 lost one layer of water and the structure was changed from type II to type I,

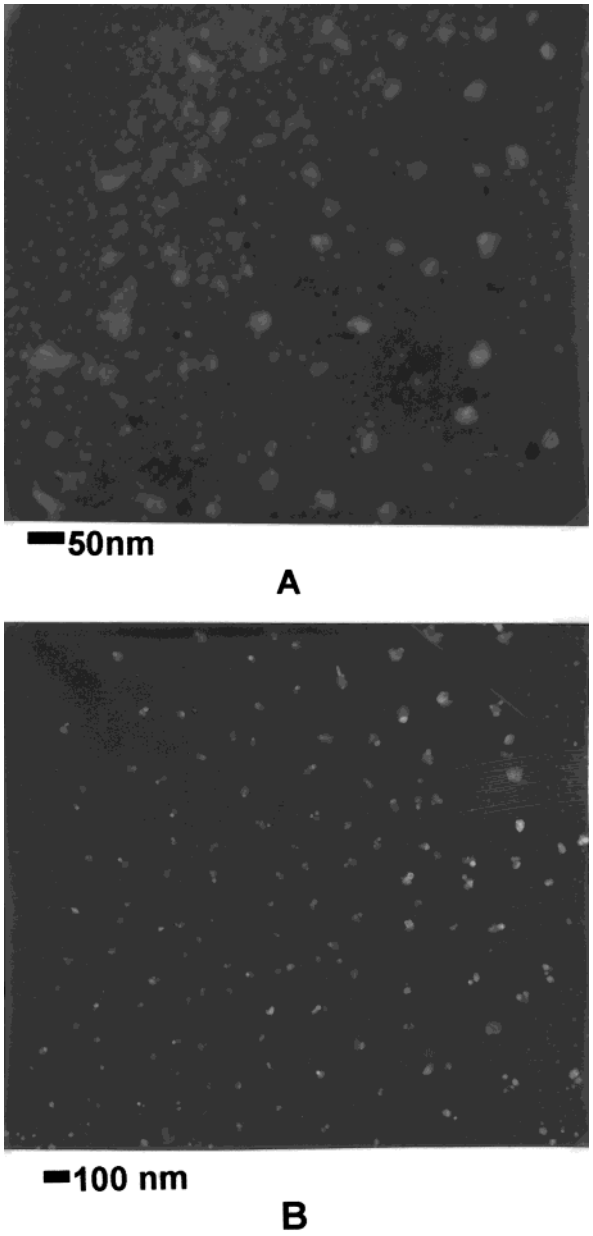

Figure 11. Transmission electron microscopy images of TPA-OL-1 nanoparticles prepared from a 0.1 M TPA manganese oxide colloid (A) 105 000 times and (B) 35 700 times.

showing that water molecules were not stable in this structure. TBA-OL-1 totally lost all TBA and most water molecules with an interlayer distance of 0.72 nm, due to weak interactions between inorganic layers and TBA. Water molecules were not stable in this structure, either. When a small amount of water was added to the dried TAA-OL-1 samples, we found their structures were the same as dried samples based on XRD data. All of the above processes are irreversible and are depicted in Figure 7.

All of the structures of DA intercalated OL-1 were stable, and the intercalated distances were the same for both wet and dried samples. Interlayer distance data show that only one layer of amines was intercalated into the layers with average intercalation angles of about 40, 69, and 61°, respectively, for en-OL-1, 1,6-DHA-OL-1, and 1,10-HOA-OL-1 (Figure 8).

These two kinds of amines are very different based on electronic and steric factors. The electrical charge of

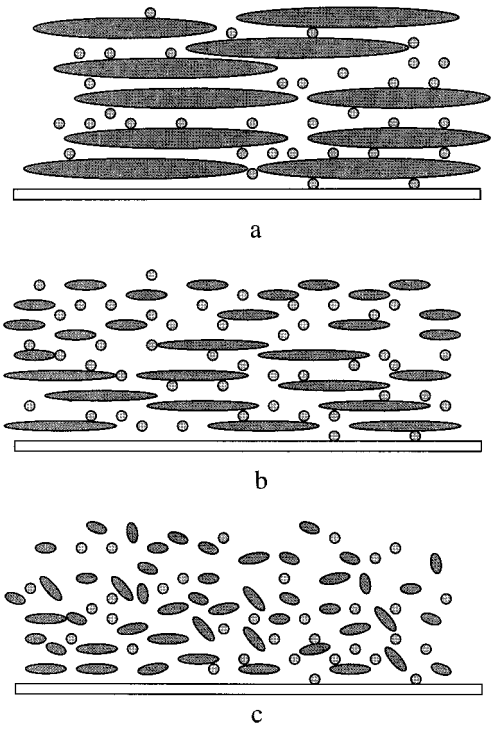

Figure 12. Schematic illustration of the ion-exchange process that takes place in the TAA-OL-1 gels at different times. (a) At the beginning formation of the gel, the H-OL-1 retained its normal particle sizes of about 20−50 μm. (b) Further intercalation of TAA ions, the stacks of layers were smaller and the particles became smaller. (c) Colloids with nanometer-sized particles of manganese oxides form after 3 days of stirring. The disks represent negatively charged disklike manganese oxide particles and the filled black circles are the tetraalkylammonium cations.

TAA is at the center of the molecule, which is covered by hydrophobic groups. DA has double the electrical charge of TAA with a distribution at both ends of the molecule, very near the negatively charged layers of OL-1, leading to very strong interactions between DA and OL-1 layers.

5. Particle Size Determination. Differences in electronic charge and steric factors not only affected the structures, but also affected particle sizes. Figures 9 and 10 show the UV−vis spectra of the colloids/sols of TAA-OL-1 and DA-OL-1, which were diluted to concentrations of 10^{-4}−10^{-3} mol L^{-1} manganese. The ICP results are listed in Table 2. One strong absorption band centered at 368 nm and one weak absorption band centered at 216 nm were found for TMA-OL-1 colloids. Based on the Beer−Lambert law, the molar absorption coefficients of TMA-OL-1 colloids with Mn concentrations of 3.60 x 10^{-5} mol L^{-1} were 2.41 x 10^{-4} and 1.89 x 10^{-4} M^{-1} cm^{-1} for the two absorption bands centered at 368 and 216 nm, respectively. Similar results were found for the other TAA-OL-1 colloids. The molar absorption coefficients of TAA-OL-1 colloids became smaller along with the longer alkyl chain TAA species intercalated into OL-1 layers. These results are similar to those of TAA manganese oxides reduced from TAA permanganate.[44]

The two higher energy electronic absorption bands of TAA-OL-1 are the result of quantum confinement effects that arise when the size of the particles becomes smaller than the electron−hole pair in the bulk semiconductor

material. The large band-gap corresponded to nanoparticle sizes of manganese oxide. TEM images of 0.1 M TAA manganese oxide colloids were obtained and are shown in Figure 11. The particle sizes are between 30 and 100 nm. Only a strong absorption band centered at 425 nm was found for en-OL-1 and a band centered at 445 nm appeared for 1,6-DHA-OL-1 and 1,10-DOA-OL-1 sols. The one strong absorption band of en-OL-1, at lower energy, showed that its particles were bigger than those of TAA-OL-1 colloids. The adsorption bands at much lower energies for 1,6-DHA-OL-1 and 1,10-DOA-OL-1 sols showed that these materials have much larger particles.

The molar absorption coefficients of TAA samples became lower as the alkyl groups of TAA ions became larger. The inorganic layers were separated by ammonium ions. These interactions between inorganic layer and ammonium ions became weaker as the chain length increased. The internal energy became smaller as the size of the TAA cations intercalated into the layers increased. Due to smaller surface areas of DA-OL-1, the molar absorption coefficients were much lower than those of TAA-OL-1 samples. The sequences of molar absorption coefficients for DA-OL-1 sols followed the same order of steric factors of diamines. The molar absorption coefficient of en-OL-1 was larger than those of 1,6-DHA-OL-1 and 1,10-DOA-OL-1 sols, due to its higher particle surface areas and shorter distances between the inorganic layers.

6. Processes in TAA-OL-1 Systems. Processes of TAA-OL-1 systems described here are quite different from our earlier research, which described a process of redox reactions between tetraalkylammonium and 2-propanol and growth of very small particles.[44] Tetraalkylammonium ions were present directly between the birnessite inorganic layers during those reactions. The systems described here are for relatively large particles of H-OL-1 materials, which were changed into nanometer-sized particles by ion-exchange methods. Figure 12 is a schematic illustration of the ion-exchange process that takes place in the TAA-OL-1 gels at different times. In the beginning of gel formation, the H-OL-1 kept its normal particle size of about 20−50 μm based on SEM analyses of H-OL-1. Further intercalation of TAA ions led to larger distances between the inorganic layers. The number of stacks of layers is smaller at the same time, because the interactions between inorganic layers and TAA ions are weaker than those between inorganic layers and K^+, H_3O^+, and DA ions. The layers are then easier to break. The particles became smaller colloids with nanometer-sized particles of manganese oxide formed after 3 days of stirring. DA-OL-1 sols had typical bulk manganese oxide character, due to strong interactions between inorganic layers and DA ions, compared with those of TAA ions.

Conclusions

Two kinds of organic amine/ammonium species (TAA and DA) were used to intercalate birnessite H-OL-1. Many kinds of novel structures were observed. Structural models are given for both wet and dry samples. The intercalation processes and stability of these systems are described. The TAA-OL-1 colloids with nanometer-sized particles were formed by ion-exchange methods. DA-OL-1 sols had typical bulk manganese oxide character.

Acknowledgment. The financial support of the Office of Basic Energy Sciences, Division of Chemical Sciences, of the U.S. Department of Energy is gratefully acknowledged.

CM000426C